Torque Measurement System Design for Step Motor 23HS30-3004S

Tran Vu Minh
School of Mechanical Engineering, Ha Noi University of Science and Technology, Hanoi, Vietnam
minh.tranvu@hust.edu.vn

Nguyen Thi Anh
Faculty of Mechanical Engineering, Thuyloi University, Vietnam
nguyenthianh200197@tlu.edu.vn

Tran Thanh Tung
Faculty of Engineering Mechanics and Automation, University of Engineering and Technology, Vietnam National University, Hanoi, Vietnam
tranthanhtung@vnu.edu.vn (corresponding author)

Received: 2 October 2024 | Revised: 4 November 2024 | Accepted: 9 November 2024

 DOI: https://doi.org/10.48084/etasr.9160

ABSTRACT

This article describes the methodology employed in the development of a prototype system designed for torque measurement. The system consists of two components. A rotating component, the transmitter, and a fixed component, the receiver. The torque data, obtained from a strain gauge bridge, are processed and transmitted to the receiver through a transformer-operated device. Rotary transformers are deployed to supply power to electronics that are mounted on shafts. This ensures continuous and stable data transmission without requiring physical connections. Additionally, the accuracy of the design model is verified through design equations and simulation results, reinforcing the system's feasibility and reliability for real-world applications.

Keywords-prototype; torque measurement; design; simulation

I. INTRODUCTION

Stepper motors are known for their ability to rotate in discrete and incremental steps [1-5]. These actuators are optimal selections for locations that necessitate accurate positioning control. In addition, synchronous motors exhibit a high torque but low-speed characteristic, which is a result of their specific design. These motors find utility in a wide range of applications, including packaging machines [6-8], fruit peeling machines [9-11], industry robots [12-16], and CNC machines [17-19]. When choosing a stepper motor, researchers often select one that meets the speed and torque requirements plus several other criteria, such as efficiency, compatibility, and durability. However, it is important to note that performance characteristics can vary significantly between different motor suppliers, even if the motors have similar specifications on paper. By analyzing the parameters provided in the motor's technical specifications, researchers can estimate the torque output at specific operating conditions, particularly when the motor is used with a compatible driver. This estimation helps ensure that the chosen motor-driver combination meets the application's performance demands under real-world conditions. This means that depending on different motor and controller combinations, different performances can be achieved from the stepper motor system. Measuring the torque from the motor is extremely important in choosing the appropriate motor for the machine design. This article presents a process for designing a torque measurement system for 23HS30-3004S stepper motors. This design aims to enable the effective application of these motors in automated systems by providing accurate and reliable torque data, ensuring optimal performance and compatibility within various automated environments.

II. MATERIALS AND METHODS

The 23HS30-3004S stepper motor is widely utilized in industrial applications due to its cost-effectiveness, ease of use, high initial torque, low-speed capability, minimal maintenance requirements, and compatibility with open-loop control systems [20-25]. The structure of the motor is the same as other types of stepper motors. The engine includes main components, such as the Motor Shaft, Cable, Connector, Encoder, Brake, and Gearbox. The options are designed to meet specific application requirements, from specialized wiring configurations and adjustable mounting flanges to tailored shaft designs that fulfill unique mechanical needs. Customized screws are crafted for specialized functions, while custom

encoders provide precise control and feedback. Custom brake systems enhance stopping capabilities, and gearboxes are adapted to respond to different torque and speed requirements. These customization options increase the motor's versatility, making it suitable for a wide range of automated and specialized applications. Table I shows the technical specifications of the engine, along with the main parameters. The technical specifications of the Nema 23 stepper motor, featuring a frame size of 57 mm × 57 mm, are also presented. The motor has a shaft diameter of 6.35 mm and a shaft length of 21 mm, with a weight of 1050 g and a lead length of 500 mm for easy installation. With an inductance of 76 mH, a phase resistance of 1.12 Ohm, and a rated current of 3 A, the motor operates efficiently. The step angle is 1.8°, providing high precision, while the holding torque reaches 189 Ncm (267.65 oz. in), ensuring reliable load holding during operation. The Nema 23 stepper motor is an ideal choice for applications in mechatronics and automation.

TABLE I. TECHNICAL SPECIFICATION OF STEPPER MOTOR [1]

Frame Size (mm)	**Nema 23 (57 × 57)**
Shaft diameter (mm)	6.35
Shaft Length (mm)	21
Lead length (mm)	500
Weight (g)	1050
Inductance (mH)	76
Phase resistance (Ohm)	1.12
Rated current (A)	3
Step angle (Deg.)	1.8
Holding torque (Ncm)	189
Holding torque (oz.in)	267.65

A. Design Of Diagram and Torque Measurement System

The working principle of the system is illustrated in Figure 2. The system comprises two primary components, the driving unit and the driving component. The drive unit is composed of a stepper motor equipped with a driver and a controller. The driven components, namely the servo motor and servo controller, are responsible for displaying pulse parameters, rotational speed, and torque ensuring precise feedback for system optimization and control. The accuracy in displaying these parameters not only allows the operator to monitor the system's performance, but also facilitates adjustments to the operational parameters to achieve optimal efficiency and enhance the system's reliability during operation. The transmission component is propelled by a belt drive mechanism. The moment value is calculated based on the number of shaft revolutions, according to the proposed model. The controller enables the modification of both the current intensity and pulse frequency values, allowing for dynamic adjustments to the system's performance in real time. This adaptability is crucial for optimizing efficiency, responding to varying load conditions, and ensuring that the system operates within the desired parameters for different applications.

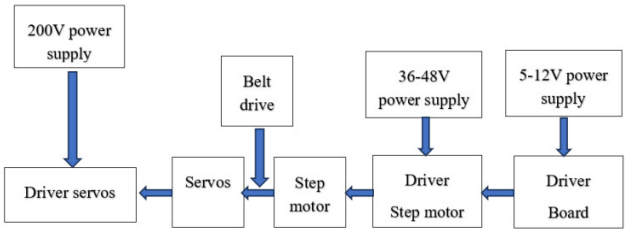

Fig. 1. Working principle of the system.

B. 3D Design Parameters

Figure 2 depicts a prototype torque measurement system for the stepper motor with the following main parts: stepper motor 23HS30-3004S, driver, belt drive, board driver, and power supply.

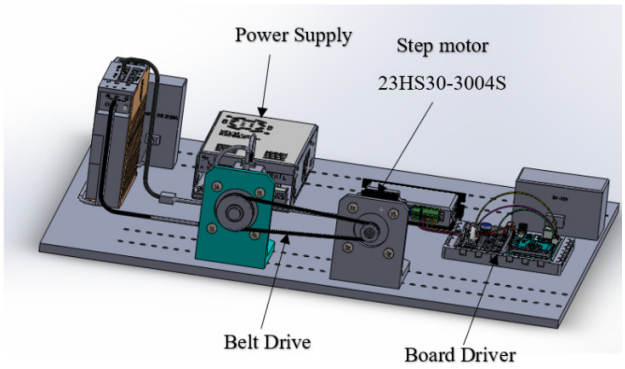

Fig. 2. Working principle of the system.

TABLE II. TECHNICAL SPECIFICATIONS OF PULLEY

Pulley	**Specification**
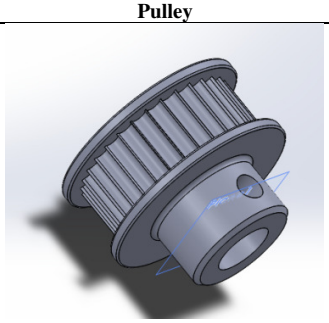	• GT2 pulley 30 teeth on 6.35 mm shaft. • Number of teeth: 30 teeth. • Tooth pitch 2 mm. • Belt width: 6 mm type. • Outer diameter: 21.5 mm. • Gear diameter: 18.5 mm. • Height: 17 mm. • Aluminum material. • Location: On the stepper motor shaft.
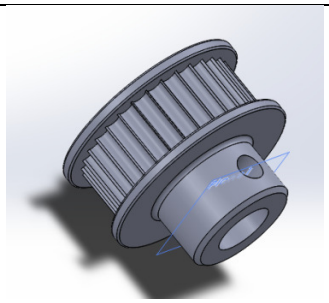	• Material: aluminum. • Number of teeth: 60. • Tooth width: 7 mm. • Outside diameter: 42. • Gear diameter: 37.8 mm. • Shaft: 14 mm. • Location: On the servo motor shaft.

C. Design of Bels Drive

Driver pulley: Torque T= 0.63 Nm, n_1 =1000 rpm.

Driven pulley:

P= 0.2 kW, n_2 = 500 rpm.

Select the number of teeth on the driver pulley: $Z_1 = 30$.

$$Z_2 = \frac{n_1.z_1}{n_q} = \frac{30\times1000}{500} = 60 \quad (1)$$

Distance between two shafts:

$$a_{min} \le a \le a_{max} \quad (2)$$

$$a_{min} = 0.5 \times m \times (Z_1 + Z_2) + 2 \times m = 0.5 \times 3 \times (30 + 60) + 2 \times 3 = 141\ (mm)$$

$$a_{max} = 2 \times m \times (Z_1 + Z_2) = 2 \times 3(60 + 30) = 540\ (mm)$$

$$a = 150\ (mm)$$

and Z_d can be calculated as:

$$Z_d = \frac{2a}{p} + \frac{Z_1+Z_2}{2} + \frac{(Z_2-Z_1)^2}{40a} \times p \quad (3)$$

where m = 3 and p =9.42.

$$Z_d = \frac{2.150}{9.42} + \frac{60+30}{2} + \frac{(60-30)^2}{40.150} \times 9.42 = 78.26 \quad (4)$$

and $Z_d = 80$ mm and $l_d = 800$ mm then:

$$a = \left(\lambda + \sqrt{\lambda^2 - 8\Delta^2}\right)/4 \quad (5)$$

where: $\lambda = l_d - \frac{p(Z1+Z2)}{2} = 329.7$ and $\Delta = m \times (Z_2 - Z_1)/2 = 45$

$$a = \frac{\left(\lambda + \sqrt{\lambda^2 - 8\Delta^2}\right)}{4} = \frac{329.7 + \sqrt{329.7^2 - 8.45^2}}{4} = 158\ (mm) \quad (6)$$

Diameter of two pulleys:

d_1=m×Z_1 = 3×30 =90 (mm).

d_2=m×Z_2 = 3×60 =180 (mm).

The number of teeth on the driven pulley can be calculated as:

$$Z_0 = Z_1.\frac{\alpha}{360^\circ} \quad (7)$$

where:

$$\alpha = 180^\circ - \left(3.\frac{60-30}{150}\right) \times 57.3 = 147^\circ$$

$$Z_0 = Z_1.\frac{\alpha}{360} = \frac{30\times147^\circ}{360^\circ} = 12.28 \quad (8)$$

Initial tension:

$$Fo = (1.1\text{:}\ 1.3)Fv = (1.1\text{:}\ 1.3)mbv^2$$

where m is the mass per unit length of the belt and b is the width of the belt.

Velocity of the belt:

$$V = \frac{\pi Dn}{1000} = \frac{3.14\times6.35\times1000}{6000} = 3.33\ (m/s) \quad (9)$$

$$Fo = (1.1\text{:}\ 1.3)Fv = (1.1\text{:}\ 1.3)mbv^2 = 0.004 \times 1.3 \times 16 \times 3.32 = 0.9\ (N)$$

Length of belts:

$$L = 2.158 + 3.14.(21 + 10.75) + \frac{(21-10.75)^2}{158} = 400\ (mm) \quad (10)$$

Based on the parameters calculated above, the GT2 pulley motor was chosen based on the specific technical specifications depicted in Table II. The specifications of the GT2 pulley are designed for a 6.35 mm shaft. This pulley features 30 teeth, with a tooth pitch of 2 mm, and a belt width of 6 mm. The outer diameter measures 21.5 mm, while the gear diameter is 18.5 mm, and its height is 17 mm. Made from aluminum, this pulley is mounted directly on the stepper motor shaft, ensuring efficient power transmission and movement.

III. RESULTS AND DISCUSSION

To induce rotation in the stepper motor, it is necessary to generate pulses. The 23HS30-3004S motor is a bipolar type of motor that has 4 wires. These 4 wires will be connected to the Driver according to the instructions provided in Figure 3.

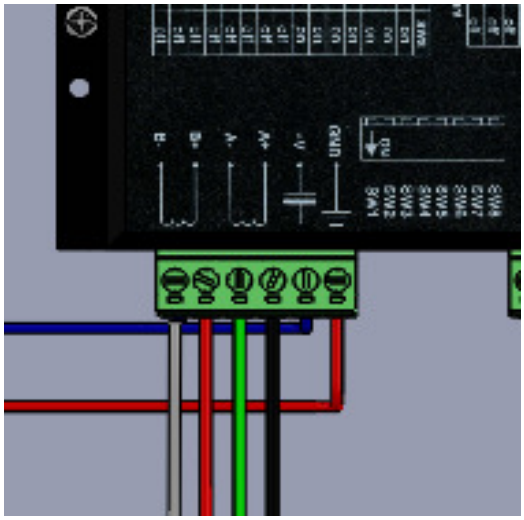

Fig. 3. Driver connect.

The current study presents the pulse generation from the control circuit with the driver to deliver/delivering pulse signals to the rotating motor, as shown in Figure 3. For the rotation speed to be modified using a transformer, the servo motor must be connected to the CN1 port of the MR -J2S-20A driver on the driver side, ensuring that it is connected via the encoder. Additionally, power is provided to the servo motor by connecting it to the MR-J2S-20A driver and activating the servo driver. The belt transmission allows for the stepper motor to transfer motion to the servo motor, enabling the measurement of the maximum revolutions and pulses. The MR-J2S-20A display screen provides visibility of these two parameters. Figure 4 illustrates the torque curve obtained from both the manufacturer's mechanical characteristics [1] and the

simulation using the proposed measurement model. Based on the obtained results, it can be inferred that an increase in the maximum static moment is related to an increase in electric current. This relationship suggests that as the electric current rises, the torque generated by the motor also increases, thereby enhancing the system's capability to handle higher loads. Consequently, optimizing the electric current can lead to improved performance and efficiency of the overall system, particularly in applications requiring significant torque output. The findings indicate that the measurement outcomes obtained from the proposed model closely resemble those obtained from the experiment. This demonstrates the reliability of the proposed model in accurately measuring torque from motors across various specific scenarios, making it suitable for efficient implementation in automated machinery. Moreover, the model's adaptability to different operating conditions ensures that it can maintain precision in diverse applications, ranging from industrial robotics to automotive systems. By effectively capturing torque data, the model not only enhances performance monitoring, but also aids in predictive maintenance, reducing downtime and operational costs. Its robust design provides engineers and operators with valuable insights, enabling them to make informed decisions that enhance system efficiency and longevity.

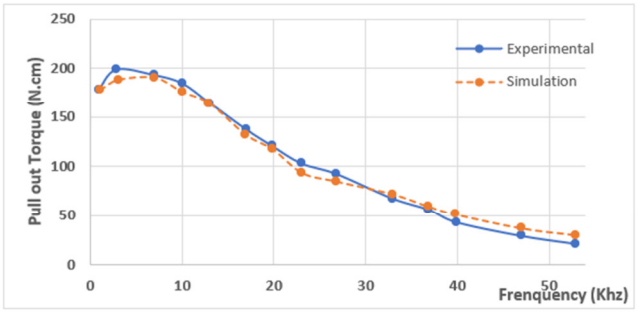

Fig. 4. Comparison between from manufacturer's mechanical characteristics and simulation [1].

IV. CONCLUSIONS

This article presents a framework for quantifying the rotational force generated by stepper motors. The calculation and design processes are thoroughly elucidated. The measurement results obtained from the model are both plausible and dependable. These reliable measurement results facilitate the accurate determination of values for system controllers, ensuring that the controllers operate within optimal parameters. Additionally, this framework enhances motor selection efficiency for automated machines by providing clear insights into the performance characteristics of various stepper motors. As a result, engineers can make informed decisions when selecting motors, ultimately leading to improved system performance and reliability in automated applications.

REFERENCES

[1] "Nema 23 Bipolar 1.8deg 1.89Nm(267.65oz.in) 3A 57x57x76mm 4 Wires - 23HS30-3004S | StepperOnline." https://www.omc-stepperonline.com/nema-23-bipolar-1-8deg-1-9nm-269oz-in-3a-3-36v-57x57x76mm-4-wires-23hs30-3004s.

[2] "Big Torque Dewo 57hs76-3004 Nema23 Stepping Motor Nema 23 Stepper Motor - Buy Stepper Motor,Nema 23,Cnc Nema23 Stepping Motor Nema 23 Stepper Motor Nema 23 High Torque Product on Alibaba.com," *www.alibaba.com*. https://www.alibaba.com/product-detail/Big-torque-DEWO-57HS76-3004-nema23_60530577451.html.

[3] M. Hojati and A. Baktash, "Hybrid stepper motor with two rows of teeth on a cup-shaped rotor and a two-part stator," *Precision Engineering*, vol. 73, pp. 228–233, Jan. 2022, https://doi.org/10.1016/j.precisioneng.2021.09.006.

[4] Z. Xu, C. Huang, H. Wang, D.-H. Lee, and F. Zhang, "Mathematical model of stepped rotor type 12/14 bearingless switched reluctance motor based on maxwell stress method," *Energy Reports*, vol. 9, pp. 556–566, Sep. 2023, https://doi.org/10.1016/j.egyr.2023.04.345.

[5] M. Hojati and A. Baktash, "Design and fabrication of a new hybrid stepper motor with significant improvements in torque density," *Engineering Science and Technology, an International Journal*, vol. 24, no. 5, pp. 1116–1122, Oct. 2021, https://doi.org/10.1016/j.jestch.2021.01.016.

[6] S. Comari *et al.*, "Mobile cobots for autonomous raw-material feeding of automatic packaging machines," *Journal of Manufacturing Systems*, vol. 64, pp. 211–224, Jul. 2022, https://doi.org/10.1016/j.jmsy.2022.06.007.

[7] S. Arunkumar, K. Suganeswaran, N. Nithyavathy, and V. K. Gobinath, "Semi-automatic cloth bag making machine," *Materials Today: Proceedings*, vol. 33, pp. 3454–3457, Jan. 2020, https://doi.org/10.1016/j.matpr.2020.05.353.

[8] T. Vu Minh, V. Cong Thiet, and T. Thanh Tung, "Design of an automated plastic bag packaging machine," *Acta Tecnología*, vol. 9, no. 1, pp. 35–38, Mar. 2023, https://doi.org/10.22306/atec.v9i1.166.

[9] F. Wang, Y. Ding, W. Xie, and D. Yang, "Design and experimental study of a separating machine for seed and peel of camellia oleifera fruit," *IFAC-PapersOnLine*, vol. 52, no. 30, pp. 87–91, Jan. 2019, https://doi.org/10.1016/j.ifacol.2019.12.502.

[10] T. V. Minh and T. T. Tung, "A Prototype of Automated Chayote Peeling Machine," *ANNUAL JOURNAL OF TECHNICAL UNIVERSITY OF VARNA, BULGARIA*, vol. 6, no. 2, pp. 83–93, Dec. 2022, https://doi.org/10.29114/ajtuv.vol6.iss2.285.

[11] V. M. Tran and T. T. Tran, "Design and Fabrication of Apple Peeling Machine," *International Journal of Mechanical and Production Engineering Research and Development (IJMPERD)*, vol. 10, no. 3, pp. 16495–16502, Jan. 2020.

[12] H. K. Dave, M. D. Chanpura, S. J. Kathrotiya, D. D. Patolia, D. D. Dodiya, and P. S. Kharva, "Design, Development and Control of SCARA for Manufacturing Processes," in *Recent Advances in Manufacturing Modelling and Optimization*, Singapore, 2022, pp. 551–567, https://doi.org/10.1007/978-981-16-9952-8_47.

[13] T. T. Tung, N. Van Tinh, D. T. Phuong Thao, and T. V. Minh, "Development of a prototype 6 degree of freedom robot arm," *Results in Engineering*, vol. 18, Jun. 2023, Art. no. 101049, https://doi.org/10.1016/j.rineng.2023.101049.

[14] S. Zhen, M. Ma, X. Liu, F. Chen, H. Zhao, and Y.-H. Chen, "Model-based robust control design and experimental validation of SCARA robot system with uncertainty," *Journal of Vibration and Control*, vol. 29, no. 1–2, pp. 91–104, Jan. 2023, https://doi.org/10.1177/10775463211042178.

[15] T. T. Tung, N. X. Quynh, and T. V. Minh, "A prototype of auto badminton training robot," *Results in Engineering*, vol. 13, Mar. 2022, Art. no. 100344, https://doi.org/10.1016/j.rineng.2022.100344.

[16] C. Urrea, J. Cortés, J. Pascal, C. Urrea, J. Cortés, and J. Pascal, "Design, construction and control of a SCARA manipulator with 6 degrees of freedom," *Journal of applied research and technology*, vol. 14, no. 6, pp. 396–404, Dec. 2016, https://doi.org/10.1016/j.jart.2016.09.005.

[17] T. T. Tung, N. X. Quynh, and T. V. Minh, "Development and Implementation of a Mini CNC Milling Machine," *Acta Marisiensis. Seria Technologica*, vol. 18, no. 2, pp. 24–28, Dec. 2021, https://doi.org/10.2478/amset-2021-0014.

[18] P. Elmiawan, D. Dharmanto, A. S.w, M. F. M, and A. R, "Akurasi Mesin Cnc Router Low Budget Berbasis Mach 3," *ROTOR*, vol. 15, no. 2, pp. 70–75, Nov. 2022, https://doi.org/10.19184/rotor.v15i2.34645.

[19] J. Veeramony and M. N. O. Zahid, "A Customizable Controller for 3 Axis Modular CNC Machine," *Journal of Modern Manufacturing Systems and Technology*, vol. 6, no. 2, pp. 55–62, Sep. 2022, https://doi.org/10.15282/jmmst.v6i2.8567.

[20] Y. Zhang, L. Wernicke, W. Wulff, A. Bleicher, and T. Schauer, "Design and validation of a dual-functional damper based on a stepper motor for energy harvesting and vibration control," *Mechanical Systems and Signal Processing*, vol. 200, Oct. 2023, Art. no. 110568, https://doi.org/10.1016/j.ymssp.2023.110568.

[21] Y. Lv, C. Xu, H. Guo, and Y. Liu, "Research on Sliding Mode Control of Two-phase Hybrid Stepper Motor Based on New PI Current Algorithm," *Journal of Physics: Conference Series*, vol. 1449, no. 1, Jan. 2020, Art. no. 012043, https://doi.org/10.1088/1742-6596/1449/1/012043.

[22] Z. Xu, Q. Yu, Y. Zhang, D.-H. Lee, and F. Zhang, "Optimization design of stepped rotor type bearingless switched reluctance motor," *Energy Reports*, vol. 9, pp. 604–612, Sep. 2023, https://doi.org/10.1016/j.egyr.2023.04.339.

[23] G. S. Gupta, P. R. Tripathi, S. Kumar, S. Ghosh, and R. K. Sinha, "Prototype design for bidirectional control of stepper motor using features of brain signals and soft computing tools," *Biomedical Signal Processing and Control*, vol. 71, Jan. 2022, Art. no. 103245, https://doi.org/10.1016/j.bspc.2021.103245.

[24] A. V. Churkin, Yu. V. Ganziy, and V. B. Dementev, "Stepper motor control system based on the ZET 7160-s module and the ZETLAB SCADA system," *Procedia Structural Integrity*, vol. 32, pp. 277–283, Jan. 2021, https://doi.org/10.1016/j.prostr.2021.09.039.

[25] J. A. Borja, I. Alvarado, and D. M. de la Peña, "Low cost two-wheels self-balancing robot for control education powered by stepper motors," *IFAC-PapersOnLine*, vol. 53, no. 2, pp. 17518–17523, Jan. 2020, https://doi.org/10.1016/j.ifacol.2020.12.2660.

[26] V.-T. Nguyen and T. T. Tung, "Design and Development of a Wheelchair Prototype," *Engineering, Technology & Applied Science Research*, vol. 14, no. 2, pp. 13376–13379, Apr. 2024, https://doi.org/10.48084/etasr.6851.

[27] P. Ubare and D. N. Sonawane, "Performance Assessment of the BLDC Motor in EV Drives using Nonlinear Model Predictive Control," *Engineering, Technology & Applied Science Research*, vol. 12, no. 4, pp. 8901–8909, Aug. 2022, https://doi.org/10.48084/etasr.4976.

[28] T. T. Tung, T. M. Tan, and T. V. Minh, "A Laser Cutting Machine Prototype," *Engineering, Technology & Applied Science Research*, vol. 14, no. 1, pp. 12944–12949, Feb. 2024, https://doi.org/10.48084/etasr.6733.